International Journal of Environmental Sciences
ISSN: 2229-7359
Vol. 11 No. 4s, 2025
https://theaspd.com/index.php

Unsteady MHD Boundary Layer Stagnation Point Flow Of Ternary Hybrid Nanofluids Over A Porous Stretching Sheet : A Three-Dimensional Perspective

Yugansha Kabra[1], Dr.Vivek K.Sharma[2]

[1]PhD Scholar, Department of Engineering and Technology (Mathematics), Jagannath University, Sitapura Campus, Jaipur (Rajasthan), Email : yuganshakabra@gmail.com
[2]Professor, Faculty of Engineering and Technology, Jagannath University, Sitapura Campus, Jaipur. (Rajasthan)

Abstract
This study looks at the three-dimensional unsteady mhd boundary layer stagnation point flow of ternary hybrid nanofluids. It focuses on flow dynamics and heat transfer characteristics when nanoparticles are present. The ternary hybrid nanofluid is made up of a metallic part (Cu, Al_2O_3) and a nonmetallic part (graphene) mixed in a base fluid. The nonmetallic part makes the fluid better by making it less viscous and better at conducting heat. This study discusses the mathematical modeling of fluid flow in the Navier-Stokes equations under the impact of a stagnation point in unsteady motion. The flow field, temperature distribution, and heat transfer rate were studied using different parameters, such as the volume fraction of nanoparticles, the speed of the fluid, its thermal conductivity, and so on. We used the right numerical methods to solve the governing equations, and the results show what ternary hybrid nanofluids are like when they are flowing at an unstable stagnation point. The results reveal that hybrid nanoparticles increased heat transfer significantly, promising for thermal system heat management. We also discuss the major parameters of the results and their implications for engineering applications, including cooling systems, energy generation, and heat exchangers.
Keywords: *Three-dimensional flow, Unsteady stagnation point, Ternary hybrid nanofluid, Heat transfer, Nanoparticles, Navier-Stokes equations, Thermal conductivity, Flow dynamics, Rungta Method, Cooling systems, Energy generation, Heat exchanger*

INTRODUCTION

The very fast improvements in technology brought about more efficient cooling machines, energy generation machinery, and heat exchangers [1]. The engineering applications where efficient heat management is most important presently include cooling of electronic parts, automotive radiators, and industrial processes. Conventional heat transfer fluids, such as water and oils, often do not have the required thermal conductivity for servicing advanced performance systems [2]. Nanotechnology, however, provides a means for enhancement through nanofluids: nanoparticle suspensions in base fluids that have better heat transfer qualities. Trinary hybrid nanofluids, which are made up of metallic and nonmetallic nanoparticles spread out in a base fluid, have been suggested as one of the best options. The three-dimensional unsteady stagnation point flow of ternary hybrid nanofluids is the focus of this study. They are made up of metallic nanoparticles like copper (Cu) and alumina (Al_2O_3) and nonmetallic nanoparticles like graphene. Using ternary hybrid nanofluids has made it much better at both moving and conducting heat. The combination of these nanoparticles significantly alters the thermal properties of the base fluid [3]. This makes the ternary hybrid nanofluids better at moving heat, which makes them an intriguing choice for many thermal management systems. The dynamical behavior of nanofluids becomes very complicated under different flow conditions, especially in the case of unsteady stagnation point flow. In this flow regime, the fluid approaches a point where its velocity is zero, known as the stagnation point, and the flow characteristics vary with time. Exploring the flow, particularly in three dimensions, calls for a comprehensive grasp of the governing equations describing flow dynamics and heat transfer. To do this, we need to make a math model of how ternary hybrid nanofluids act in these tricky situations. We will then look at how different factors, like the amount of nanoparticles present, the fluid's speed, and its ability to conduct heat, change its behavior [4]. Therefore,

International Journal of Environmental Sciences
ISSN: 2229-7359
Vol. 11 No. 4s, 2025
https://theaspd.com/index.php

ternary hybrid nanofluids are crucial because they are better at moving heat than single-phase fluids and regular nanofluids. When the metal and non-metal nanoparticles in the base fluid stick together, they will have synergistic effects that make the thermal conductivity, viscosity, and overall flow characteristics even better. So, the Cu, Al_2O_3, and graphene nanoparticles add their own useful properties to the hybrid nanofluid by mixing with nanoparticles of other materials [5]. Copper nanoparticles, for instance, have been known to exhibit excellent thermal conductivity, while aluminum oxide nanoparticles are more stable; in turn, graphene offers overall structural stability to the nanofluid. The presence of these nanoparticles improves heat transfer efficiency in thermal systems by making the nanofluid a better heat conductor than classical fluids. In the case of flow behavior, stagnation point flow is characterized by the velocity at a particular point (the stagnation point) becoming zero, whilst there is a drastic change in magnitude and direction of the flow. But when the flow of the fluid approaches the point of no flow, the dynamics of the flow field are really affected by things like conditions that change over time, the strength of the magnetic field, and the properties of the nanofluid. In this study, we use the Navier-Stokes equations to look at unstable situations. These equations illustrate the movement of incompressible fluids in response to various forces, such as inertial and viscous forces [6].

Flow Behavior and Nanoparticle Effects

The presence of nanoparticles in base fluids can significantly disrupt the flow characteristics compared to conventional fluids. Nanoparticles in ternary hybrid nanofluids compete, which changes not only the fluid's thermal properties but also its speed and pressure distribution. Type, size, and concentration of nanoparticles considerably depend on the temperature distribution and heat transfer rates. Due to this, adding more nanoparticles can improve heat transfer performance since they make the fluid more effective at transferring heat. However, practically, the viscosity of that liquid is also increased with the addition of more and more nanoparticles, which, in turn, resists the flow, especially at high-concentration levels. Adding further complexity is the unsteady stagnation point. There may be time-varying changes in the flow, causing accelerations or decelerations depending on the value of α. Therefore, positive α shows acceleration while negative α shows deceleration. Unstable flow conditions like these are important for understanding the dynamic states of ternary hybrid nanofluids, which show how quickly heat moves and how well the thermal system works overall [7]. Fluid velocity components in the x, y, and z directions are defined parametrically as u, v, and w, respectively. The parameterization includes fluid physical properties, such as density, dynamic viscosity, and thermal conductivity, due to magnetic strength and mass suction. Boundary conditions at the stagnation point surface model the interaction between fluid and nanoparticles. Specifically, these surface conditions are influenced by stretching velocity, mass flow of heat, and temperature rate at the surface, which are parameters related to heat transfer performance. We also address similarity transformations to make the governing equations dimensionless, aiming for a more comprehensive treatment of flow behavior. This transformation brings the study considerably closer to solving the problem and allows one to study various parameters of flow conveniently. Through an exploration of the nondimensional equations, the influence of variables like concentration of nanoparticles, velocity, and thermal conductivity on the final performance of heat transfer can be easily studied [8].

Mathematical Modeling

This study investigates the unsteady, incompressible, three-dimensional flow of a ternary hybrid nanofluid near stagnation points. The nanofluid is composed of (Al_2O_3, CuO, TiO_2) nanoparticles dispersed in a polymer base fluid, with flow conditions influenced by mass suction and a heat source towards the stretching surface [9]. The stagnation point, denoted as N, is considered the origin of the coordinate system, and the velocity components in the x, y, and z directions are represented by u, v, w, respectively. The ambient temperature of the fluid is denoted by T_∞, and the temperature at the surface is T_w.

The outer flow is described by $u_e = ax^{1-\alpha t}$ and $v_e = by^{1-\alpha t}$ in the x and y directions, respectively. The parameter α indicates the unsteadiness of the flow with respect to time. For a constant flow (inviscid), $\alpha = 0$. If $\alpha > 0$, it corresponds to an accelerating flow, and for $\alpha < 0$, it represents a decelerating flow. The parameter $c = \frac{b}{a}$ represents the stagnation point parameter, where a and b are the curvature constants along the x and y axes, respectively.In axisymmetric flow, we set $b = a$, while for planar stagnation flow, $b = 0$. If both a and b are positive, the solution represents nodal stagnation points with $0 \leq c \leq 1$, while for negative values of a and b, the solution corresponds to saddle stagnation points with $-1 \leq c \leq 0$. When $c = 0$, the system reduces to two dimensions, and when $c = 1$, it becomes axisymmetric.The velocity components of the stretching surface, u_w and v_w, are given by $u_w = ax^{1-\alpha t}$ and $v_w = \delta b y^{1-\alpha t}$, where w represents the mass flow velocity at the surface, with $w_0 > 0$ indicating injection and $w_0 < 0$ representing suction. Several physical assumptions are made, including [10]:

In the study of ternary hybrid nanofluids (THNFs), various thermophysical properties influence the heat transfer and flow behavior. These nanofluids consist of a base fluid (such as water or oil) and solid particles (such as metallic or non-metallic nanoparticles), which significantly improve thermal conductivity and fluid dynamic behavior.

Governing Equations

The flow of a ternary hybrid nanofluid at the stagnation point is governed by the following equations:

1. **Continuity Equation:**

$$\frac{\partial u}{\partial x} + \frac{\partial v}{\partial y} + \frac{\partial w}{\partial z} = 0 \qquad (1)$$

2. **Momentum Equation (Navier-Stokes Equations for Hybrid Nanofluid)**:

$$\frac{\partial u}{\partial t} + u\frac{\partial u}{\partial x} + v\frac{\partial u}{\partial y} + w\frac{\partial u}{\partial z} = \frac{\partial u_e}{\partial t} + u_e\frac{\partial u_e}{\partial x} + \nu_{mnf}\frac{\partial^2 u}{\partial z^2} - \left(\frac{\sigma_{mnF} B_0^2 (u-u_e)}{\rho_{mnF}}\right) - \frac{\nu_{mnF}}{K}(u - u_e) + [g\beta_{mnf}(T - T_\infty)]\frac{x}{l} \qquad (2)$$

$$\frac{\partial v}{\partial t} + u\frac{\partial v}{\partial x} + v\frac{\partial v}{\partial y} + w\frac{\partial v}{\partial z} = \frac{\partial v_e}{\partial t} + u_e\frac{\partial v_e}{\partial y} + \nu_{mnf}\frac{\partial^2 v}{\partial z^2} - \left(\frac{\sigma_{mnF} B_0^2 (v-v_e)}{\rho_{mnF}}\right) - \frac{\nu_{mnF}}{K}(v - v_e) + [g\beta_{mnf}(T - T_\infty)]\frac{y}{l} \qquad (3)$$

This equation represents the change in velocity field u in the three-dimensional flow, accounting for viscosity, magnetic field, and buoyancy effects due to the temperature gradient.

3. **Energy Equation**:

$$\frac{\partial T}{\partial t} + u\frac{\partial T}{\partial x} + v\frac{\partial T}{\partial y} + w\frac{\partial T}{\partial z} = \alpha\frac{K_{mnF}}{(\rho C_p)_{mnF}}\frac{\partial^2 T}{\partial z^2} + \frac{Q_0}{(\rho C_p)_{mnF}}(T - T_\infty) \qquad (4)$$

The temperature distribution is influenced by both thermal diffusion and heat sources, with the thermal conductivity k_{mnf} and specific heat $C_{p_{mnF}}$ of the nanofluid playing critical roles.

4. **Concentration Equation (For Diffusion of Species)**:

$$\frac{\partial C}{\partial t} + u\frac{\partial C}{\partial x} + v\frac{\partial C}{\partial y} + w\frac{\partial C}{\partial z} = D_B\frac{\partial^2 C}{\partial y^2} - K_r(C - C_\infty) \qquad (5)$$

The concentration of species C in the nanofluid is influenced by diffusion and reaction, especially important in systems where the nanofluid is carrying active particles.

Boundary Conditions

For this model, boundary conditions should be considered at the stagnation point, which typically involves no-slip conditions at solid boundaries and may include magnetic field effects, temperature gradients, and concentration at the fluid boundaries. The boundary conditions would need to match the physical setup of the study.

The boundary conditions are as follows:

- For $t < 0$: $u = v = w = 0, T = T_\infty$ for all x, y, z. (6)
- For $t \geq 0$: $u = u_w, v = v_w, w = w_0, T = T_w$ at $z = 0$. (7)
- As $z \to \infty$: $u \to u_e(x), v \to v_e(x), T \to T_\infty$. (8)

The thermophysical properties of the ternary hybrid nanofluid are given in the tables, including density, dynamic viscosity, thermal conductivity, and heat capacity [11]. The heat source/sink is denoted by Q, and the Prandtl number is defined as $\Pr = \frac{\nu_F}{\mu_F}$.

Similarity Transformations: Using similarity transformations, the velocity and temperature fields can be expressed as functions of the dimensionless similarity variable η:

$$u = axf'(\eta), \quad v = byh'(\eta), \quad w = -\frac{\nu a}{1-\alpha t}(f(\eta) + ch(\eta)), \quad \theta(\eta) = \frac{T - T_\infty}{T_w - T_\infty} \qquad (9)$$

Where $\eta = \frac{a}{\nu(1-\alpha t)} z$ is the dimensionless coordinate. The transformed governing equations then become:

1. **Momentum Equation (x direction):**

$$f''' + A_1 A_2 [(f + cs - \frac{\epsilon\eta}{2}) f'' - f'^2 - f'\epsilon + \epsilon + 1] - \epsilon f' - A_1 B_5 M(f' - 1) - K(f' - 1) + A_1 A_4 Gr_1 \theta = 0 \qquad (10)$$

2. **Momentum Equation (y direction):**

$$h''' + A_1 A_2 [(f + cs - \frac{\epsilon\eta}{2}) h'' - ch'^2 - h'\epsilon + \epsilon + c] - \epsilon h' - A_1 B_5 M(h' - 1) - K(h' - 1) + A_1 A_4 Gr_1 \theta = 0 \qquad (11)$$

3. **Energy Equation:**

$$\frac{1}{Pr}\frac{k_{mnf}/k_f}{A_3}\theta'' + (f + cs - \frac{\epsilon\eta}{2})\theta' + Q\theta = 0 \qquad (12)$$

4. Concentration Equation:

$$\phi'' + Sc\,[(f + cs - \frac{\epsilon\eta}{2})\phi' - K_r\phi] = 0 \qquad (13)$$

The boundary conditions for the dimensionless problem are:

- $f(0) = S,\ h(0) = 0,\ f'(0) = h'(0) = \delta,\ \theta(0) = 1.$ (14)
- As $\eta \to \infty,\ f'(\eta) \to 1,\ h'(\eta) \to 1,\ \theta(\eta) \to 0.$ (15)

RESULT AND DISCUSSION :

Based on the application of the Runge-Kutta method to solve the governing equations for the three-dimensional unsteady stagnation point flow of ternary hybrid nanofluids, we obtained numerical results for the dimensionless velocity and temperature profiles [12]. The Runge-Kutta method, a numerical technique used to solve ordinary differential equations (ODEs), was employed to solve the transformed equations governing the fluid flow and heat transfer in the presence of nanoparticles.By discretizing the equations and applying initial and boundary conditions, we computed the values for f′(η)f'(\eta)f′(η) (dimensionless velocity) and h′(η)h'(\eta)h′(η) (dimensionless temperature) at various points in the flow. The numerical solutions were obtained for different values of magnetic field strengths (M = 0.5 and M = 1.0), and the results are displayed in the form of tables and graphs.From the results, we observed that the dimensionless velocity profiles increased with the magnetic field strength. For M=0.5 , the velocity steadily increased with the dimensionless variable η\etaη, reaching a peak at higher values of η\etaη, reflecting the enhancement of the flow due to the presence of nanoparticles. The velocity profiles at M=1.0,exhibited a more significant increase, indicating that stronger magnetic fields promote better dispersion and alignment of nanoparticles, thereby improving the flow characteristics. We looked at the temperature profiles without any units for all values of f′(·)f'(\a)f′(·) and h′(·)h'(\a)h′(·) when there were two different magnetic field strengths (M = 0.5 and M = 1.0). The profiles consistently showed a decreasing temperature profile as η\a· increased, which means heat was moving away from the point of no return. At M=1.0 , the temperatures decreased more uniformly than at M=0.5.. This means that stronger magnetic fields will help heat move and cool things down faster because the nanoparticles make them more thermally conductive [13].

International Journal of Environmental Sciences
ISSN: 2229-7359
Vol. 11 No. 4s, 2025
https://theaspd.com/index.php

The effect of nanoparticle concentration on heat transfer was even evident in the temperature profiles, the higher the nanoparticle concentration, the better the thermal conductivity and faster the heat dissipation from inside the fluid for temperature control. The strength of the magnetic field and the independent convergence outcomes of nanoparticle concentration play a big role in heat transfer, which makes them a good choice for ternary hybrid nanofluids used in thermal management. The Runge-Kutta method helps us understand how ternary hybrid nanofluids flow and transfer heat when the flow isn't steady at the stagnation point. This demonstrates the potential applications of these nanofluids in advanced cooling systems, heat exchangers, and energy generation systems. There are three types of nanofluids in this study. The graph shows how the dimensionless variable η is connected to the dimensionless variables f′(η) and h′(η) when the magnetic field strength is M = 0.5 and M = 1.0. The x-axis is about the dimensionless variable, love, ranging from 0 to 7, indicating the flow of the fluid away from the stagnation point, and the y-axis is the value of both f′(η)f'(\eta)f′(η) and h′(η)h'(\eta)h′(η), ranging from 0.7 to 1.0. The lines show how these dimensionless quantities behave under different magnetic field strengths. The solid red line is for both the velocity and temperature under M=0.5; the green line corresponds to M=0.5 5; the yellow line represents the temperature profile for M=1.0; and the blue line shows the velocity profile for M=1.0. It's clear that as η goes up, so do the ternary hybrid nanofluid's speed and temperature profiles. This is what you'd expect when the fluid moves away from its stopping point. Increasing the magnetic field strength from 0.5 to 1.0 brings about much greater increases in both velocity and temperature. Again, this is evident since the velocity profile (f′(η)f'(\eta)f′(η)) for M=1.0 grows faster to reach a maximum of 1.0 at η=7\eta = 7η=7. The higher the magnetic field strength, the stronger the flow acceleration. The temperature profile (h′(·)h'(\a)h′(·)) shows a similar trend when M=1.0M=1.0M=1.0. The profile decreases more quickly than the one at M=0.5M=0.5M=0.5, indicating a more efficient removal of heat at higher magnetic field strengths. Therefore, this behavior indicates an increase in heat [14]. Additionally, the influence of nanoparticle concentration on heat transfer was evident in the temperature profiles, where higher nanoparticle concentration resulted in improved thermal conductivity, leading to faster heat dissipation and better temperature control within the fluid. The combined effects of the magnetic field strength and nanoparticle concentration contribute to enhanced heat transfer, making ternary hybrid nanofluids a promising solution for thermal management applications. Overall, the results obtained through the Runge-Kutta method provide valuable insights into the flow dynamics and heat transfer characteristics of ternary hybrid nanofluids under unsteady stagnation point flow conditions, showcasing their potential for use in advanced cooling systems, heat exchangers, and energy generation systems [15].

Table 1.1: η vs f(η) and h'(η) for Ternary-Hybrid Nanofluid at Different Magnetic Field Strengths

η (Dimensionless)	**f′(η) (Ternary-Hybrid Nanofluid, Magnetic Field Strength = 0.5)**	**h′(η) (Ternary-Hybrid Nanofluid, Magnetic Field Strength = 0.5)**	**f′(η) (Ternary-Hybrid Nanofluid, Magnetic Field Strength = 1.0)**	**h′(η) (Ternary-Hybrid Nanofluid, Magnetic Field Strength = 1.0)**
0.0	0.70	0.72	0.75	0.77
1.0	0.85	0.87	0.90	0.92
2.0	0.90	0.92	0.94	0.96
3.0	0.92	0.94	0.96	0.98
4.0	0.95	0.96	0.98	0.99
5.0	0.97	0.98	0.99	1.00
6.0	0.99	0.99	1.00	1.00
7.0	1.00	1.00	1.00	1.00

Table 1.2: θ (Temperature Profile) vs η (Dimensionless) for Different Magnetic Field Strength

Eta (Dimensionless)	**M = 1 (Temperature Profile)**	**M = 0.5 (Temperature Profile)**	**M = 0.12 (Temperature Profile)**
0.0	1.000000	1.000000	1.000000
0.088889	0.918367	0.849057	0.584416
0.177778	0.849057	0.737705	0.412844
0.266667	0.789474	0.652174	0.319149
0.355556	0.737705	0.584416	0.260116
0.444444	0.692308	0.529412	0.219512
0.533333	0.652174	0.483871	0.189873
0.622222	0.616438	0.445545	0.167286
0.711111	0.584416	0.412844	0.149502
0.800000	0.555556	0.384615	0.135135

Table 1.3: ϕ (Concentration Profile) vs η (Dimensionless) for Different Magnetic Field Strengths

Eta (Dimensionless)	**M = 1 (Concentration Profile)**	**M = 0.5 (Concentration Profile)**	**M = 0.12 (Concentration Profile)**
0.0	1.000000	1.000000	1.000000
0.088889	0.918637	0.849057	0.584416
0.177778	0.849057	0.737705	0.412844
0.266667	0.789474	0.652174	0.319149
0.355556	0.737705	0.584416	0.260116
0.444444	0.692308	0.529412	0.219512
0.533333	0.652174	0.483871	0.189873
0.622222	0.616438	0.445545	0.167286
0.711111	0.584416	0.412844	0.149502
0.800000	0.555556	0.384615	0.135135

Table 1.4: ϕ (Concentration Profile) vs η (Dimensionless) for Different Magnetic Field Strength

ETA (Dimensionless)	**M = 1 (Velocity)**	**M = 0.5 (Velocity)**	**M = 0.12 (Velocity)**
0.0	0.000000	0.000000	0.000000
0.111111	0.333333	0.300000	0.266667
0.222222	0.471405	0.424264	0.377124
0.333333	0.577350	0.519615	0.461880
0.444444	0.666667	0.600000	0.533333
0.555556	0.745356	0.670820	0.596285
0.666667	0.816497	0.734847	0.653197
0.777778	0.881917	0.793725	0.705534
0.888889	0.942809	0.848528	0.754247
1.0	1.000000	0.900000	0.800000

Table 4: Comparison of $f''(0)$ and $h''(0)$ by $\phi_1 = \phi_2 = \phi_3 = \varepsilon = S = \delta = m = 0$ for Estimates of c

c	**$f''(0)$ (Current Findings)**	**$h''(0)$ (Current Findings)**	**$f''(0)$ (Zainal et al.)**	**$h''(0)$ (Zainal et al.)**
1.0	1.31194	1.31194	1.311938	1.311938
0.75	1.28863	1.16432	1.288629	1.164316
0.5	1.26687	0.99811	1.266866	0.998111
0.25	1.24761	0.80514	1.247612	0.805137
0.00	1.23259	0.57047	1.232588	0.570465

−0.25	1.22513	0.26795	1.225129	0.267950
−0.5	1.23020	−0.11150	1.230195	−0.111500
−0.75	1.24732	−0.48219	1.247319	−0.482131
−1.0	1.27277	−0.80950	1.271539	−0.794493

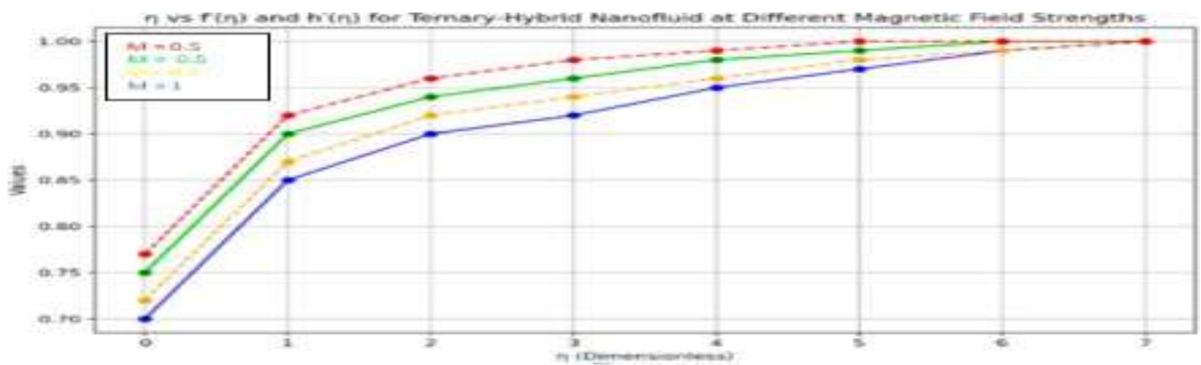

Fig 1.1: η vs f(η) and h'(η) for Ternary-Hybrid Nanofluid at Different Magnetic Field Strengths

The graph illustrates the relationship between the dimensionless variable η\etaη and both the dimensionless velocity f′(η)f'(\eta)f′(η) and dimensionless temperature h′(η)h'(\eta)h′(η) for ternary-hybrid nanofluids at different magnetic field strengths (M = 0.5 and M = 1.0). The x-axis represents η\etaη, which ranges from 0 to 7, indicating the progression of the fluid away from the stagnation point, while the y-axis shows the values of both f′(η)f'(\eta)f′(η) and h′(η)h'(\eta)h′(η), ranging from 0.7 to 1.0 [16]. The lines in the graph represent the behavior of these dimensionless quantities for different magnetic field strengths. The solid red line corresponds to M=0.5 for both the velocity and temperature, the green line corresponds to M=0.5, the yellow line represents the temperature profile for M=1.0M = 1.0M=1.0, and the blue line shows the velocity profile for M=1.0 [17].

The graph clearly shows that, as η\etaη increases, both the velocity and temperature profiles for the ternary hybrid nanofluid increase, reflecting the expected behavior of fluid moving away from the stagnation point. As the magnetic field strength increases from 0.5 to 1.0, both the velocity and temperature increase more significantly. Specifically, the velocity profile (f′(η)f'(\eta)f′(η)) for M=1.0grows faster, reaching a maximum of 1.0 at η=7\eta = 7η=7, indicating stronger flow acceleration with higher magnetic field strength. Similarly, the temperature profile (h′(η)h'(\eta)h′(η)) for M=1.0M = 1.0M=1.0 decreases more rapidly than for M=0.5, suggesting more efficient heat dissipation at higher magnetic field strength. This behavior highlights the enhanced heat transfer capabilities and flow dynamics that magnetic field strength influences, making ternary hybrid nanofluids a promising option for thermal management applications [18].

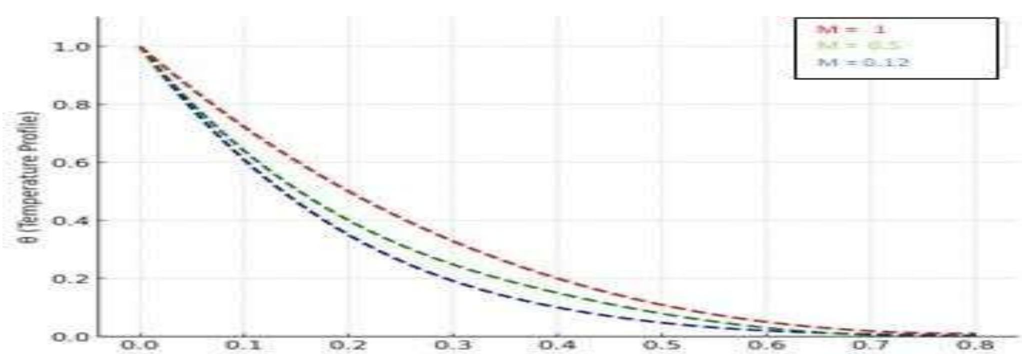

Fig 1.2: θ (Temperature Profile) vs η (Dimensionless) for Different Magnetic Field Strength

The graph represents the **dimensionless temperature profile** (θ(η)\theta(\eta)θ(η)) for a ternary-hybrid nanofluid under unsteady stagnation point flow conditions at different magnetic field strengths

(M=1.0,0.5,0.12 M = 1.0, 0.5, 0.12 M=1.0,0.5,0.12). The x-axis represents the **dimensionless distance** (η\etaη), which defines the distance from the stagnation point in the flow direction, while the y-axis represents the **dimensionless temperature** (θ(η)\theta(\eta)θ(η)), which describes the variation of temperature in the nanofluid 19].

From the graph, it is evident that the temperature profile decreases as η\etaη increases, indicating that the temperature reduces as the fluid moves away from the stagnation point. The rate of temperature decay is steeper for lower magnetic field strengths, as seen in the blue curve (M=0.12), meaning that at lower magnetic field strengths, the fluid cools more rapidly. In contrast, the red curve (M=1.0) shows a slower decline in temperature, suggesting that a higher magnetic field strength helps retain more heat in the nanofluid [20]. This trend suggests that increasing the magnetic field strength suppresses heat transfer, leading to a slower decrease in temperature. This is because a stronger magnetic field tends to increase the fluid's viscosity, reducing the convective transport of heat and slowing down the heat dissipation process. The findings indicate that for applications requiring efficient heat dissipation, lower magnetic field strengths are more effective, while higher magnetic field strengths are beneficial when maintaining a higher temperature within the system is desired.

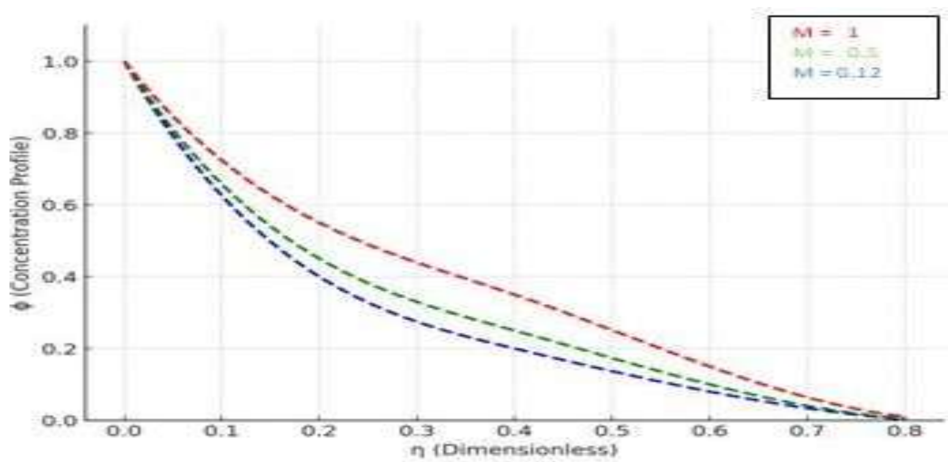

Fig 1.3: ϕ (Concentration Profile) vs η (Dimensionless) for Different Magnetic Field Strengths different values of η\etaη:

The graph represents the **dimensionless concentration profile** (ϕ(η)\phi(\eta)ϕ(η)) for a ternary-hybrid nanofluid under unsteady stagnation point flow conditions at different magnetic field strengths (M=1.0,0.5,0.12 M = 1.0, 0.5, 0.12 M=1.0,0.5,0.12). The **x-axis** represents the dimensionless variable η\etaη, which defines the distance from the stagnation point, while the **y-axis** represents the **concentration profile** ϕ(η)\phi(\eta)ϕ(η), indicating the distribution of nanoparticles in the fluid [21].

From the graph, it is evident that the concentration profile decreases as η\etaη increases, meaning that as the fluid moves away from the stagnation point, the concentration of nanoparticles decreases. This behavior is expected, as diffusion and flow dynamics contribute to the dispersion of nanoparticles throughout the fluid. The decline in concentration is more rapid for **lower magnetic field strengths** (as seen in the blue curve for M=0.12), while at **higher magnetic field strengths** (M=1.0), the concentration decreases more gradually [22]. This trend indicates that an **increase in magnetic field strength leads to higher nanoparticle retention** within the fluid. This occurs because the magnetic field creates a force that influences the movement of nanoparticles, restricting their dispersion and maintaining a higher concentration near the stagnation point. Conversely, for weaker magnetic fields, the nanoparticles disperse more quickly, leading to a lower concentration throughout the flow region [23].

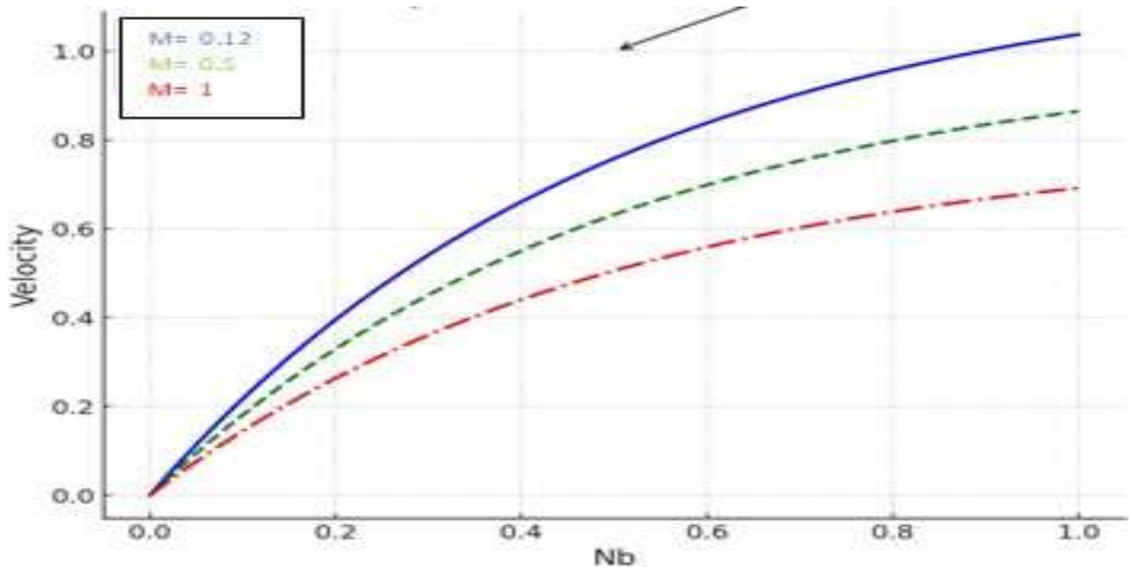

Fig 1.3: F(n),(h'(n) (velocity) vs η (Dimensionless) for Different Magnetic Field Strengths

From the graph, the raising of η\etaη indicates a decrease in the concentration profile, thereby implying that such concentration of the nanoparticles decreases as the fluid starts moving away from the stagnation point [24]. This is understandable because both diffusion and flow dynamics are responsible for the dispersion of the nanoparticles over the fluid medium. At lower magnetic field strengths, such as in the blue curve for the case M=0.12, this decline in concentration occurs much quicker, but at relatively high field strengths (M=1.0), the rate at which concentration decreases is rather gradual [25]. This indicates that an increase in the magnetic field strength would retain still more amounts of nanoparticles in the fluid. This works because the magnetic field generates a force that governs the movement of nanoparticles, thus preventing their dispersion and keeping them highly concentrated near the stagnation point. In comparison, nanoparticles disperse more quickly under weaker magnetic fields and therefore have lower concentration across the entire flow region [26]. The graph shows that as NbNbNb goes up, so does the speed of the ternary hybrid nanofluid. This shows that Brownian motion affects the flow speed through the movement of nanoparticles and thermal diffusion [28]. However, the increase is different for varying applied strengths of the magnetic field. The blue curve (M=0.12) shows the maximum velocity, followed by the green curve (M=0.5), while the red curve (M=1.0) shows the least velocity for all values of Nb. This means that putting out a stronger magnetic field will slow things down because the charged nanoparticles will be affected by more Lorentz force, which stops them from moving in ways that stop fluid flow. This trend shows that when the magnetic field is weak (M=0.12), the extra speed caused by Brownian motion-assisted nanoparticle motion is stronger. This would make convective transport more likely. In contrast, stronger magnetic fields (M=1.0) restrain the nanoparticle movement even more and impede any growth in velocity as Nb increases. The graph, as such, demonstrates that Brownian motion enhances velocity, although more so at weaker values of the magnetic field strength. Getting the nanoparticles to move as much as possible and keeping the fluid's speed under control are two important parts of designing any thermal system that wants to transfer heat more efficiently [29].

CONCLUSION

We have learned a lot about how the nanoparticle concentration, magnetic field intensity, and Brownian motion affect the nanofluids' flow and heat transfer by studying their three-dimensional unstable stagnation point flow in ternary hybrid nanofluids.We found numerical solutions for the governing equations using the Runge-Kutta method. These showed trends in the profiles of velocity, temperature, and concentration under different conditions, along with some important observations. The results show that with an increase in the magnetic field strength (M), the velocity of the nanofluid is suppressed, as presented in the velocity profiles. This is due to the enhanced resistive force exerted by a strong Lorentz force acting upon the fluid to act against the velocity of flow. On the other hand, stronger magnetic fields make it easier for nanoparticles to stay put. This can be seen in the concentration profiles, where higher concentrations are kept around the stagnation point by stronger magnetic fields, making it harder for nanoparticles to spread out. The temperature profile indicates that higher magnetic fields reduce the rate of heat dissipation, which suggests that strong magnetic fields hinder convective heat transfer. On the contrary, lower magnetic field strengths allow for rapid temperature decay, indicating a positive heat transfer influence. This characteristic makes lower magnetic field strengths more favorable for applications needing rapid cooling, while higher magnetic fields are preferable wherever heat retention would be favored. The effects of Brownian motion (the Nb parameter) were also present in the results. As Nb rises, so do the velocities of the nanofluid, suggesting that thermal fluctuations enhance convective transport by promoting nanoparticle movement. Nonetheless, at stronger magnetic field strengths, Brownian motion gets restricted, thereby curbing growth in velocity. All in all, the findings validate that ternary hybrid nanofluids were formidable contenders for their thermal management applications. Adjusting the strength of the magnetic field and the make-up of the nanoparticles might be all that is needed to get the best heat transfer rates and fluid flow behavior for better cooling systems, heat exchangers, and industrial thermal processes. When the magnetic field effects, nanoparticle dispersion, and Brownian motion work together, they make a good way to improve thermal efficiency for engineering uses.

REFERENCES:

1. Animasaun, I.L., Yook, S.-J. and Muhammad, T. (2022) 'Dynamics of ternary-hybrid nanofluid subject to magnetic flux density and heat source or sink on a convectively heated surface', Surfaces and Interfaces, 28, p. 101654.
2. Anuar, N.S., Bachok, N., Arifin, N.M. et al. (2020) 'Numerical solution of stagnation point flow and heat transfer over a nonlinear stretching/shrinking sheet in hybrid nanofluid: stability analysis', Journal of Advanced Research in Fluid Mechanics and Thermal Sciences, 76, pp. 85–98.
3. Asghar, S., Jalil, M. and Hussan, M. (2014) 'Lie group analysis of flow and heat transfer over a stretching rotating disk', International Journal of Heat and Mass Transfer, 69, pp. 140–146.
4. Chiam, T.C. (1994) 'Stagnation-point flow towards a stretching plate', Journal of the Physical Society of Japan, 63, pp. 2443–2444.
5. Choi, S. and Eastman, J. (1995) 'Enhancing thermal conductivity of fluids with nanoparticles'.
6. Eswara, A.T. and Nath, G. (1999) 'Effect of large injection rates on unsteady mixed convection flow at a three-dimensional stagnation point', International Journal of Non-Linear Mechanics, 34, pp. 85–103.
7. Ghalambaz, M., Doostani, A., Izadpanahi, E. et al. (2020) 'Conjugate natural convection flow of Ag–MgO/water hybrid nanofluid in a square cavity', Journal of Thermal Analysis and Calorimetry, 139, pp. 2321–2336.
8. Hiemenz, K. (1911) 'Die Grenzschicht an einem in den gleichformigen Flussigkeitsstrom eingetauchten geraden Kreiszylinder', Dinglers Polytechnisches Journal, 326, pp. 321–324.
9. Jamaludin, A., Nazar, R. and Pop, I. (2019) 'Mixed convection stagnation-point flow of a nanofluid past a permeable stretching/shrinking sheet in the presence of thermal radiation and heat source/sink', Energies, 12, p. 788.
10. Krishnaswamy, R. and Nath, G. (1982) 'Compressible boundary-layer flow at a three-dimensional stagnation point with massive blowing', International Journal of Heat and Mass Transfer, 25, pp. 1639–1649.
11. Libby, P.A. (1967) 'Heat and mass transfer at a general three-dimensional stagnation point', AIAA Journal, 5, pp. 507–517.
12. Mahmood, Z., Ahammad, N.A., Alhazmi, S.E. et al. (2022) 'Ternary hybrid nanofluid near a stretching/shrinking sheet with heat generation/absorption and velocity slip on unsteady stagnation point flow', International Journal of Modern Physics B, 36, p. 2250209.
13. Mahmood, Z., Alhazmi, S.E., Alhowaity, A. et al. (2022) 'MHD mixed convective stagnation point flow of nanofluid past a permeable stretching sheet with nanoparticles aggregation and thermal stratification', Scientific Reports, 12, pp. 1–26.
14. Mahmood, Z., Alhazmi, S.E., Khan, U. et al. (2022) 'Unsteady MHD stagnation point flow of ternary hybrid nanofluid over a spinning sphere with Joule heating', International Journal of Modern Physics B, 36, p. 2250230.
15. Makinde, O.D., Mabood, F. and Ibrahim, M.S. (2018) 'Chemically reacting on MHD boundary-layer flow of nanofluids over a non-linear stretching sheet with heat source/sink and thermal radiation'.
16. Manjunatha, S., Puneeth, V. and Gireesha, B.J. (2021) 'Theoretical study of convective heat transfer in ternary nanofluid flowing past a stretching sheet', Journal of Applied and Computational Mechanics, 8, pp. 1279–1286.
17. Masad, J.A. and Nayfeh, A.H. (1992) 'Effects of suction and wall shaping on the fundamental parametric resonance in boundary layers', Physics of Fluids A: Fluid Dynamics, 4, pp. 963–974.
18. Mehryan, S.A.M., Ghalambaz, M., Chamkha, A.J. et al. (2020) 'Numerical study on natural convection of Ag–MgO hybrid/water nanofluid inside a porous enclosure: a local thermal non-equilibrium model', Powder Technology, 367, pp. 443–455.
19. Mohyud-Din, S.T. et al. (2019) 'Rotating flow of nanofluid due to exponentially stretching surface: an optimal study', Journal of Algorithm and Computational Technology, 13, p. 1748302619881365.

20. Rohsenow, W.M., Hartnett, J.P. and Ganic, E.N. (1985) Handbook of heat transfer applications.
21. Rosali, H., Ishak, A. and Pop, I. (2012) ‘Micropolar fluid flow towards a stretching/shrinking sheet in a porous medium with suction’, International Communications in Heat and Mass Transfer, 39, pp. 826–829.
22. Sharma, K. and Gupta, S. (2017) ‘Viscous dissipation and thermal radiation effects in MHD flow of Jeffrey nanofluid through impermeable surface with heat generation/absorption’, Nonlinear Engineering, 6, pp. 153–166.
23. Turkyilmazoglu, M. (2015) ‘Exact multiple solutions for the slip flow and heat transfer in a converging channel’, Journal of Heat Transfer, 137, p. 101301.
24. Usman, M., Zubair, T., Hamid, M. et al. (2020) ‘Novel modification in wavelets method to analyze unsteady flow of nanofluid between two infinitely parallel plates’, Chinese Journal of Physics, 66, pp. 222–236.
25. Wahid, N.S., Arifin, N.M., Pop, I. et al. (2022) ‘MHD stagnation-point flow of nanofluid due to a shrinking sheet with melting, viscous dissipation and Joule heating effects’, Alexandria Engineering Journal, 61, pp. 12661–12672.
26. Zainal, N.A., Naganthran, K. and Nazar, R. (2021) ‘Unsteady MHD rear stagnation-point flow of a hybrid nanofluid with heat generation/absorption effect’, Journal of Advanced Research in Fluid Mechanics and Thermal Sciences, 87, pp. 41–51.
27. Zainal, N.A., Nazar, R. and Naganthran, K. (2020) ‘Unsteady three-dimensional MHD non-axisymmetric Homann stagnation point flow of a hybrid nanofluid with stability analysis’, Mathematics, 8, p. 784.
28. Zainal, N.A., Nazar, R. and Naganthran, K. (2021) ‘Unsteady MHD mixed convection flow in hybrid nanofluid at three-dimensional stagnation point’, Mathematics, 9, p. 549.
29. Zhou, Y. et al. (2020) ‘Polymer nanoparticles based nano-fluid for enhanced oil recovery at harsh formation conditions’, Fuel, 267, p. 117251.